Taylor & Francis
Taylor & Francis Group

Journal of Macromolecular Science, Part B
Physics

ISSN: 0022-2348 (Print) 1525-609X (Online) Journal homepage: http://www.tandfonline.com/loi/lmsb20

Prediction of Spherulite Size in Rotationally Molded Polypropylene

J. A. Martins , M. C. Cramez , M. J. Oliveira & R. J. Crawford

To cite this article: J. A. Martins , M. C. Cramez , M. J. Oliveira & R. J. Crawford (2003) Prediction of Spherulite Size in Rotationally Molded Polypropylene, Journal of Macromolecular Science, Part B, 42:2, 367-385

To link to this article: http://dx.doi.org/10.1081/MB-120017125

MARCEL DEKKER, INC. • 270 MADISON AVENUE • NEW YORK, NY 10016

JOURNAL OF MACROMOLECULAR SCIENCE®
Part B—Physics
Vol. B42, No. 2, pp. 367–385, 2003

Prediction of Spherulite Size in Rotationally Molded Polypropylene

J. A. Martins,[1,*] M. C. Cramez,[1] M. J. Oliveira,[1] and R. J. Crawford[2]

[1]Departamento de Engenharia de Polímeros, Universidade do Minho, Guimarães, Portugal
[2]School of Mechanical Engineering, Queen's University, Belfast, UK

ABSTRACT

Rotational molding is used to manufacture hollow plastic parts. It is characterized by relatively slow cooling rates, which leads to large spherulites and brittleness in rotomolded polypropylene parts. Using both theoretical and experimental methods, this article assesses the factors that control spherulite size so that the properties of rotationally molded polypropylene parts can be improved. The approach taken is to predict the average density of the nuclei of isothermally crystallized polypropylene as a function of the crystallization temperature, using data on the half-time of crystallization (determined by differential scanning calorimetry) and the spherulite growth rate (measured by optical microscopy). The prediction method is then extended to nonisothermal quiescent crystallization, such as occurs in rotational molding, by determining the temperature corresponding to half of the phase change and its relationship with the cooling rate. To establish the average true sample temperature on cooling, experimental data are corrected for the temperature calibration at a particular cooling rate, the thermal resistance of the sample, and the release of the heat of crystallization. The surface nuclei density of polypropylene specimens, as crystallized isothermally and nonisothermally in differential scanning calorimetry, and also as processed by rotational molding, was determined by optical microscopy and converted

*Correspondence: J. A. Martins, Universidade do Minho, Departamento de Engenharia de Polímeros, Campus de Azurém, 4800–058 Guimarães, Portugal; Fax: 351 + 253 + 510249; E-mail: jamartins@dep.uminho.pt.

DOI: 10.1081/MB-120017125
0022-2348 (Print); 1525-609X (Online)

www.dekker.com

MARCEL DEKKER, INC. • 270 MADISON AVENUE • NEW YORK, NY 10016

to volume density using the Voronoy relationship. A good agreement was found to exist between the experimental results and the predictions.

Key Words: Spherulite size; Prediction; Polypropylene; DSC; Optical microscopy; Rotational molding.

INTRODUCTION

The importance of the dimensions of the crystalline structure on the mechanical properties of materials has been well documented. In the metallurgical field, more specifically in the field of steel making, a parameter of great practical interest is the *grain size number* (G), defined in the metric system as $G_m = (\log_{10} m/\log_{10} 2) - 2.95$, where m is the number of grains per square millimeter at $1\times$ magnification.[1] For austenitic steels, at low temperatures, the yield strength follows a Hall-Petch law being inversely proportional to the square root of the grain size, while for high temperatures the dependence is on the aspect ratio of the grains.[2]

For polymers, it is also known that materials crystallized at high temperatures, where the semicrystalline structures are larger and "more perfect," have lower failure strains than materials crystallized at lower temperatures, with smaller and less perfect semicrystalline structures.[3,4] It is not clear whether the spherulite size, the lamella thickness, the crystallinity degree, or the tie molecules play the main role in failure behavior. There is, however, clear evidence of a relationship between lamellae thickness and spherulite size, both being of importance in the establishment of many important properties of molded plastic parts.

This is particularly true for plastic parts produced by rotational molding, which have relatively large spherulites and classical morphologies.[5] This processing technique involves heating plastic powder in a rotating metal mold until it coats its inside surface, followed by a cooling period with the mold still rotating until the part sets. What makes this process quite distinct from other common processing methods, such as injection molding, is that the heating and cooling rates are slow, typical of the order of 10°C/min. Also, in most commercial molding situations, heating and cooling occur from only one side of the part. Previous work on the rotational molding of polypropylene[6] showed that the size of the spherulites increases from the surface that contacts the mold wall (fast cooling) toward the interior of the molding (slower cooling), with consequential effects on the mechanical properties and shape of the part. In the case of rotomolded semicrystalline polymers, crystallization occurs under almost quiescent conditions, and representative temperature gradients can be reproduced in laboratory equipment, such as differential scanning calorimetry (DSC).

In this work, a previously developed methodology, which relates the data obtained by DSC and optical microscopy to predict the density of nuclei in polymers crystallized isothermally with instantaneous nucleation,[7] is extended to nonisothermal crystallization, also under quiescent conditions and further applied to rotational molding.[8] The errors related to the application of the method, either to isothermal and nonisothermal crystallization, are analyzed and discussed. In particular, the true sample temperature in nonisothermal DSC scans, is evaluated by doing a calibration on cooling and taking into

account the sample thermal resistance and the release of the heat of crystallization during solidification.

THEORY

Prediction of the Average Density of Nuclei for Isothermal Crystallization

There are two ways to predict the average density of nuclei from isothermal crystallization data. One makes combined use of half of the crystallization time ($t_{50\%}$) and the spherulite growth rate (G). The other makes use of G and the kinetic constant (k) obtained from the best fit of single-stage equations, such as Avrami's equation, to the experimental data.

Half of the crystallization time, $t_{50\%}$, is obtained from isothermal DSC experiments, in which the measured parameter is the differential variation with time of the heat of crystallization released during the phase change. It is independent of the model chosen to describe the overall crystallization kinetics, and effects such as secondary crystallization and annealing play a minor role in its definition.

However, the relationship between $t_{50\%}$ and the spherulite growth rate (measured in a hot-stage fitted into an optical microscope) is dependent on the method used to describe the overall phase change. The most common procedure to describe the isothermal crystallization of polymers as a single-stage process is the Avrami–Evans–Komolgoroff approach.[9–11] This has the form

$$X(t) = 1 - \exp(-kt^n) \tag{1}$$

where k and n have their usual meanings, and t is the crystallization time, with $t = 0$ set at the start of the isothermal process (no induction time is assumed). X is the degree of conversion to the solid phase.

For an instantaneous nucleation of spherical particles ($n = 3$), then ($1/t_{50\%}$) is directly proportional to the linear growth rate,

$$\frac{1}{t_{50\%}} = \left(\frac{k}{\ln(2)}\right)^{1/3} = (C\bar{N})^{1/3}G \tag{2}$$

where $C = 4\pi\rho_s/[3\rho_l \ln(2)]$, $\bar{N}$ is the average number of nuclei per unit volume of untransformed material, and ρ_s and ρ_l are the densities of the solid and liquid phases, respectively. Temperature dependence of the linear growth rate of the spherulites, G, may be derived from the Lauritzen–Hoffman theory for secondary nucleation.[12] Assuming a coherent secondary surface nucleation, the linear growth rate is

$$G(T) = G_o \cdot \exp\left(-\frac{\Delta G_d}{k_B T}\right) \cdot \exp\left(-\frac{K_g}{T \cdot \Delta T \cdot f}\right) \tag{3}$$

where ΔG_d is the activation energy for the transport of the supercooled stem to the semicrystalline nuclei, T is the absolute temperature, $K_g = cb\sigma\sigma_e T_m^0/(k_B \Delta H)$, where c is 4 for regimes I and III and 2 for regime II, the other parameters have their usual meanings, ΔT is supercooling (difference between the thermodynamic melting

temperature and crystallization temperature), and f is a corrective factor for the decrease of enthalpy of fusion with the crystallization temperature.

In Eq. (2), $\bar{N}$ is assumed to be temperature independent, and the temperature dependence of $(1/t_{50\%})$ relates to the growth rate. As a result of this temperature independence, a plot of $\ln(1/t_{50\%})$ vs. $(1/T\Delta Tf)$ should be shifted from a plot of $\ln(G)$ vs. $(1/T\Delta Tf)$ by a temperature-independent constant value given by $\ln[4\pi\bar{N}\rho_s/(\ln 2{\cdot}3\rho_l)]^{1/3}$, yielding a constant density of nuclei for all crystallization temperatures.

Because it is experimentally found that the density of nucleation increases with a decrease of the crystallization temperature, which is reflected in the higher slope of a plot of $\ln(1/t_{50\%})$ vs. $(1/T\Delta Tf)$ when compared with that of $\ln(G)$ vs. $(1/T\Delta Tf)$, it is convenient to establish, even approximately, the temperature dependence of $\bar{N}$ in Eq. (2).

This temperature dependence may be established if one assumes an ideal solution of N_s segments of a chain in a favorable conformational state to be added to a semicrystalline cluster (embryo). A procedure used by Kurz and Fisher[13] to evaluate the density of nuclei in the solidification of metals was applied to the solidification of polymers.[7] A general expression for the number of embryos with critical size, assumed to be equal to the average density of nuclei per unit volume of transformed material, $\bar{N}_t$, is

$$N_e^* = \bar{N}_t = N_s \exp\left(-\frac{\Delta G_c^*}{k_B T}\right) \tag{4}$$

where ΔG_c^* is the critical energy for the activation of one embryo and $\bar{N}_t = (\rho_s/\rho_l)\bar{N}$. For a coherent heterogeneous nucleation of a rectangular nucleus with base (ab) and thickness (l) in a plane substrate, ΔG_c^* is the same as the activation energy for the formation of a secondary nucleus. Then, we may define a $K_n = 4b_o\sigma\sigma_e T_m^0/(k_B\Delta H_f^0)$, and $\bar{N}_t$ from Eq. (4) is

$$N_e^* = \bar{N}_t = N_s \exp\left(-\frac{K_n}{T\Delta T}\right) \tag{5}$$

that has the same temperature dependence as the spherulite growth rate, Eq. (3). Limitations concerning the derivation of the above equation were analyzed and discussed.[7]

Assuming now that the average number of critical embryos per unit volume is the same as the average number of nuclei, $\bar{N}_t$, the substitution of Eqs. (5) and (3) into Eq. (2) allows the definition of an apparent value for $K_g^{1/t_{50\%}} = K_{\mathrm{n}} + K_{\mathrm{g}}$. Thus, it is evident why the slope of $\ln(1/t_{50\%})$ vs. $(1/T\Delta Tf)$ is higher. $K_g^{1/t_{50\%}} > K_g^G$, where $K_g^G = K_g$ is the slope of $\ln(G)$ vs. $(1/T\Delta Tf)$. If the surface energies involved in the formation of the primary nuclei are the same as those involved in the formation of the secondary nuclei (during growth), then $K_n = K_g^G$ (for regimes I and III), and the apparent value of $K_g^{1/t_{50\%}}$ for an instantaneous nucleation of spheres should then be (4/3) $K_g^G = 1.333K_g^G$. The ratio $K_g^{1/t_{50\%}}/K_g^G$ may also be used to make inferences about the nucleation type and about the geometry of the growing structures. For coherent heterogeneous substrates, the equality between K_n and K_g^G is physically acceptable, because the surface energies involved in the formation of the primary nucleus (σ and σ_{e}) are the same as those involved in secondary nucleation.

Assuming a constant regime in the temperature range where the two pieces of experimental data are available, or in the region where they are extrapolated to, the average

density of nuclei, obtained by the substitution of Eqs. (5) and (3) into Eq. (2), and solving this equation for $\bar{N}_t$ is

$$\bar{N}_t = \frac{1}{C_t}\cdot\exp\left\{-3(K_g^{1/t_{50\%}} - K_g^G)\cdot\frac{1}{T\cdot\Delta T\cdot f} + 3\left[\ln\left(\frac{1}{t_{50\%}}\right)_o - \ln(G)_o\right]\right\} \tag{6}$$

with $C_t = (\rho_l C/\rho_s)$, as a result of the conversion to average density of nuclei per unit volume of transformed material. The ordinates at the origin, $\ln(1/t_{50\%})_o$ and $\ln(G)_o$, are evaluated by a linear fit over the DSC and optical microscopy experimental data.

Prediction of the Average Density of Nuclei for Nonisothermal Crystallization

Modeling of the nonisothermal crystallization is usually done using Nakamura's equation, which is only valid for processes with instantaneous nucleation.[14] The general form of this is

$$X(T) = 1 - \exp\left\{-\left[\int_{T_m^0}^{T} Z(T')\frac{1}{\dot{T}}\mathrm{d}T'\right]^n\right\} \tag{7}$$

where $\dot{T}$ is the cooling rate, n the Avrami index, with exactly the same physical meaning as the exponent used in isothermal crystallization kinetics. The term $Z(T')$ in the argument of the integral is related to the kinetic constant of Avrami's Eq. (1), which, for an instantaneous nucleation of spheres, $n = 3$, is

$$Z(T') = (k)^{1/3} = \left(\frac{4\pi\bar{N}}{3}\right)^{1/3}\cdot G \tag{8}$$

which is also directly proportional to the spherulite growth rate, as in the isothermal case.

Therefore, as in the isothermal crystallization case, we may define a temperature $T_{50\%}$ as the temperature at which the degree of conversion to the solid phase reaches half of its final value. It may be shown that, for $T = T_{50\%}$, $X = 0.5$, and the relationship between $T_{50\%}$ and $Z(T')$ in the Nakamura equation is

$$\frac{T_{50\%} - T_m^0}{\dot{T}} = \frac{(\ln 2)^{1/3}}{\bar{Z}(T_{50\%})} \tag{9}$$

which is similar to Eq. (2) derived for the isothermal case.

It is then assumed that the major phase change occurs in a narrow temperature interval around $T_{50\%}$, and thus the nonisothermal crystallization process may be considered as approximately isothermal. As will be shown later, this assumption is justified by the change in shape of the experimental curves resulting from the corrections for the thermal resistance of the sample and for the release of the heat of crystallization.

After evaluation of a temperature $T_{50\%}$, "equivalent" to $t_{50\%}$ in isothermal experiments, an empirical relationship between $T_{50\%}$ and the cooling rate may be established enabling, by the application of Eq. (6), the evaluation of the density of nucleation for a particular cooling rate. This method is valid for low cooling rates but, due to errors in the method by which the calibration on cooling is performed,[15] it may loose validity for high scanning rates.

The application of this method for predicting the size of the spherulites in rotational molding requires knowledge of the rate of cooling through the thickness of the part. This can be determined by direct measurement of the temperature, by means of thermocouples inserted at different positions within the part wall, or by using heat transfer equations in simulation software, such as RotoSim.[16]

Evaluation of the Average True Sample Temperature

As described previously, evaluation of the true sample temperature requires calibration of the DSC on cooling, and account must be taken of the thermal resistance of the sample and for the heat of crystallization released during the phase change.

The basics of the procedure to make these corrections are as follows. More details about the method can be found elsewhere.[15,17] At a particular scanning rate, the thermal lag between the sample and the sensor is recorded; it is the difference between the true temperature of the sample (expected melting onset) and the recorded temperature (either sensor or program temperature). This thermal lag is due to thermal resistance of the oven. Because nonisothermal experiments are transient in nature, the thermal lag is rate dependent, and it must be evaluated for each scanning rate. Assuming that the temperature sensor is perfectly calibrated for zero scanning rate experiments (zero isothermal correction), a condition that is hardly ever found, the thermal lag on cooling should be equal in magnitude and opposite in sign to that on heating.

In practice, an isothermal correction is often needed. This is the difference between the extrapolated measured temperature at zero scanning rate and the expected temperature. In contrast to the rate-dependent thermal lag, which is symmetrical for heating and cooling experiments, the isothermal correction is the same for both scanning modes. It may be positive or negative, it may change in the experimental temperature range (due to nonlinearity in the temperature reading of the thermocouple), and is device dependent. Ways to deal with this correction were discussed in detail previously.[15]

At a particular cooling rate, the true sample temperature of a pure substance, with high thermal conductivity, is

$$T_t^- = (2 - a^+)\,T_m - b^- \tag{10}$$

with $b^- = 2\Delta T_o + b^+$. T_m is the measured temperature; a^+ and b^+ are, respectively, the slope and the ordinate at the origin of the calibration line at a particular heating rate (the same as was used for cooling), and ΔT_o is the isothermal correction.

When polymer samples (or other materials with low thermal conductivity) are being analyzed, the true sample temperature is different from T_t^-. Two additional corrections are needed: one for the thermal resistance of the sample and another for the release of the heat of crystallization. Accounting for these two corrections, the average true sample temperature $(T_t^-)_s$ may be evaluated from

$$(T_t^-)_s = T_t^- + \left(|\Delta H_c| m_s R_s \frac{dX}{dt} - m_s \bar{C}_p R_s \frac{d(T_t^-)_s}{dt}\right) \tag{11}$$

where m_s is the mass of the sample, (dX/dt) is the rate of the solid-phase formation, with $t = (T_m^o - T_t^-)/|\dot{T}|$ and $|\Delta H_c|$ is the enthalpy of crystallization; $\bar{C}_p$ is the heat capacity of the sample; and R_s is thermal resistance at a particular cooling rate, dT/dt. It is assumed in Eq. (11) that the change in time of the average true sample temperature is equal to the scanning rate. Providing that a proper calibration is performed over experimental data, the temperature $(T_t^-)_s$, or (T_t^-), is independent of the recording mode.[18]

Conversion from a Surface Density to a Volume Density of Nuclei

To check the validity of the procedure described previously for predicting the average density of nuclei, either under isothermal or nonisothermal conditions, it is necessary to determine the number of nuclei, per unit area, in a section of a sample crystallized at a specified temperature. As a first approximation, the columnar (or transcrystalline) nuclei formed in the upper and lower surfaces of the samples crystallized in the DSC pans, may be neglected because their contribution to overall crystallization is small in comparison with that of the equiaxial nuclei.

A three-dimensional picture of a Poisson distribution of $\bar{N}_t$ number of nuclei, formed instantaneously, may be obtained from a Monte-Carlo simulation. For the case of interest, the statistical moment of three-dimensional Voronoy tessellations, given by Van de Weygaert,[19] is

$$\bar{\sigma} = \frac{\Gamma(1/3)(16\pi^5\bar{N}_t^2/9)^{1/3}}{15} = 1.4580\bar{N}_t^{2/3} \tag{12}$$

where $\bar{\sigma}$ is the surface density of nuclei, and Γ is the gamma function.

Other work done in the area of crystallization kinetics is that of Eder et al.[20] and Isayev et al.[21] An expression similar to Eq. (2), when this equation is solved for the density of nuclei, was presented by Eder et al.[22]

$$\bar{N}(T) = \frac{3V_\infty}{4\pi}\left[\frac{Z(T)}{G(T)}\right]^n \tag{13}$$

where V_∞ is the maximum volume fraction of spherulites at infinite time and $Z(T)$ was defined previously by Eq. (8).

Equation (13) was used by Isayev et al. to predict the density of nuclei and the average spherulite size in injection molded samples.[21] However, in his procedure, use is made of the induction time, which depends on the sensitivity of the measuring device and on the quantity being measured. Experimental data was further corrected for the thermal resistance of the sample, using a procedure conceptually similar to the one that led to Eq. (11). The Nakamura equation is then fitted to the data and the parameters of $Z(T)$ found from the best fit. After implementation of the aforementioned corrections, these investigators apparently succeed in predicting the final spherulite size as a function of the processing conditions.

We do not know of any experimental verifications made by Eder et al. to predict the average density of nuclei using Eq. (13). They had made an assessment of the volume density of nuclei from microscopic analysis of sample sections [assuming that $\bar{N}_t \cong (\bar{\sigma})^{3/2}$], which

is overestimated by a factor of $(1/1.458)^{3/2}$ [see Eq. (12)]. No comparison of this experimental nuclei density was made with the predicted value from Eq. (13).

EXPERIMENTAL

Material

The material used in this work is a rotational molding grade of polypropylene, Borealis BE 182 B, with a melt flow index of 13 g/10 min. The thermodynamic melting temperature, as measured by the Hoffman and Weeks method, was 176.75°C.

Isothermal Crystallization in the DSC

Isothermal crystallization experiments were carried out in a PerkinElmer DSC 7 (Norwalk, CT, USA). Before any experiment taking place, a calibration with two metal standards was performed at the slowest scanning rate of the device, 0.1°C/min. Samples of about 8 mg were held at 190°C for 1 min and then cooled down to the crystallization temperature at 80°C/min. The sample was held at the crystallization temperature for a time long enough to guarantee complete crystallization. Other experimental details concerning the methodology used for this experiment are described elsewhere.[7] In all the experiments, zero time was taken as the time at the start of the isothermal process.

Isothermal Crystallization in the Hot-Stage Microscope

For measurement of the spherulite growth rate, a Linkam THMS 600 hot stage coupled with an Olympus BH2 optical microscope was used. To ensure better temperature control, the hot stage was cooled with nitrogen gas, previously cooled in an ice bath. Temperature calibration of the hot stage was performed with phenacetin and checked against DSC data, also at 0.1°C/min. A deviation of 0.5°C between the optical melting temperature and the DSC onset of melting was noted.

Melt-pressed samples of powder material were heated to 190°C, held at this temperature for 3 min and then cooled at 50°C/min to the crystallization temperature. Crystallization of the samples was recorded using an Olympus BH2 optical microscope, coupled to a JVC TK1280E camera and to a Sony EVO-965OP video recorder. Measurements of the spherulites size at different times were performed using a Leica Quantimet 500 image analysis system.

Nonisothermal Crystallization in DSC

Samples of about 8 mg were held at 190°C for 1 min and then cooled at a constant rate, varying from -4 to -32°C/min. Calibration on cooling was performed from the onsets of melting of two standard metals at the same scanning rates, according to Eq. (10).

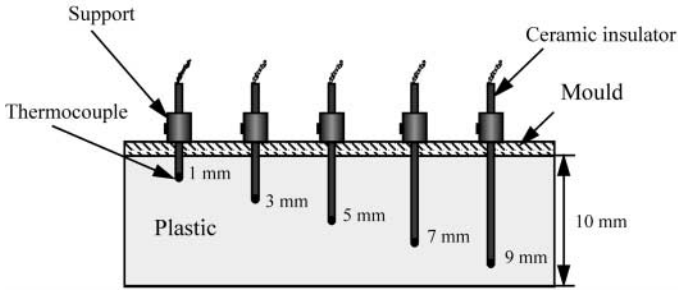

Figure 1. Thermocouple positions during the processing of a 10-mm-thick polypropylene part.

The average true sample temperature was then evaluated according to Eq. (11). The errors with which the calibration on cooling was performed were evaluated by measuring, at several scanning rates, the differences between the onsets of liquid crystalline transitions on heating and cooling.[15] The eventual rate dependence of the supercooling associated with the liquid-crystalline transition is impossible to be quantified and therefore it is included in the aforementioned errors.

Rotational Molding

A cube-shaped mold with 400 mm sides was used to prepare a 10-mm-thick part. The temperatures inside the molded part during processing were monitored using the Rotolog system.[23] Seven thermocouples were used to measure the temperatures across the part thickness, as depicted in Fig. 1. The temperature readings during cooling of the part are shown in Fig. 2.

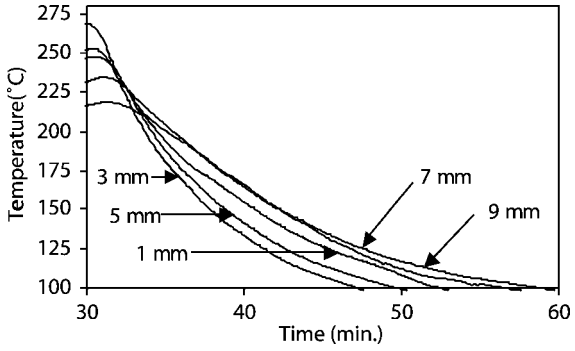

Figure 2. Temperature variation as a function of time for the different thermocouple positions of Fig. 1.

Table 1. Half of crystallization times ($t_{50\%}$), kinetic constant (k), and Avrami exponent (n) obtained from DSC data with the time set at the start of the isothermal.

T (°C)	$t_{50\%}$ (sec)	k ($\sec^{-n}$)	n	SLS $\times 10^3$
116	34.8	1.26×10^{-4}	3.72	5.63
118	50.4	8.79×10^{-5}	3.46	3.40
120	90.6	2.23×10^{-4}	2.81	0.78
122	121.2	2.04×10^{-4}	2.65	7.06
124	214.8	1.27×10^{-4}	2.46	0.89
126	301.8	1.81×10^{-6}	3.06	1.78
128	501.6	8.46×10^{-7}	2.93	0.41
130	808.8	3.01×10^{-7}	2.86	1.41

SLS is the sum of least squares between experimental data and the predictions of Avrami's equation.

Measurement of the Number of Spherulites

The number of spherulites per unit area were determined on sections cut across the rotationally molded part and also from specimens crystallized in the DSC pans. Sections were cut with a Leitz 1401 microtome with a thickness of about 12 μm, immersed in Canada balsam and observed under the polarized light microscope. The two-dimensional results obtained were converted to the correspondent three-dimensional values using Eq. (12).

RESULTS

The results for half the crystallization time obtained from the DSC experiments, together with the constant values obtained with Avrami's equation, are shown in Table 1.

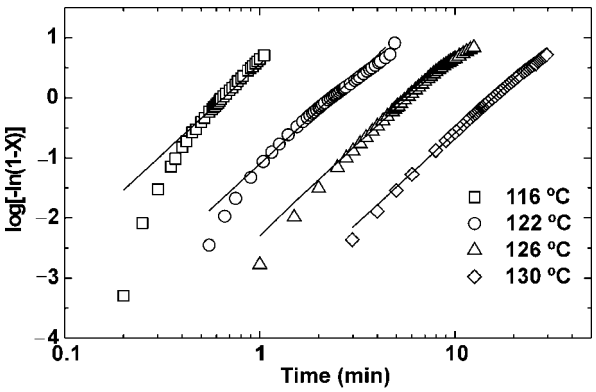

Figure 3. Isothermal crystallization of polypropylene at the indicated temperatures and fit with Avrami equation with $n = 3$ for all crystallization temperatures.

Table 2. Spherulite growth rate of polypropylene crystallized in the hot stage at the indicated temperatures.

T (°C)	120	122	124	126	128	130	132
G (μm/sec)	1.124	0.858	0.576	0.388	0.258	0.176	0.161

The description of the isothermal crystallization of the polypropylene using Avrami's equation is good, with a sum of least squares of the order of 10^{-3}. An Avrami exponent near 3 was obtained for all crystallization temperatures.

Because of the derivation of Eq. (6) and the application of the Voronoy equation [Eq. (12)], it is implicit that there is an instantaneous nucleation and growth of perfect spheres, the description of the isothermal crystallization was performed at several temperatures with Avrami's equation and n constant at 3 (Fig. 3). The sum of least squares obtained by the fitting of this equation with experimental data is similar in magnitude to the previous one shown in Table 1.

The experimental results for the growth rate of the spherulites at several crystallization temperatures are shown in Table 2. These results, together with those of the reciprocal half of crystallization times are plotted as a function of $(1/T\Delta Tf)$ in Fig. 4. From the growth rate data (open circles), it is assumed that a constant regime exists in the temperature range studied. The absolute value of the slope of the $\ln(G)$ line in Fig. 4 is $2.689 \times 10^5\,\mathrm{K}^2$ and that of $\ln(1/t_{50\%})$ is $3.368 \times 10^5\,\mathrm{K}^2$. The ratio of these two slopes, $K_g^{1/t_{50\%}}/K_g^G$, is 1.253, which is near to the expected theoretical value of 1.333 for an instantaneous nucleation of perfect spheres. Also in Fig. 4, the dotted line is a plot of the kinetic constant $\ln(k^{1/3})$ from Avrami's equation against $(1/T\Delta Tf)$, which follows closely the result of $\ln(1/t_{50\%})$, according to Fig. 3.

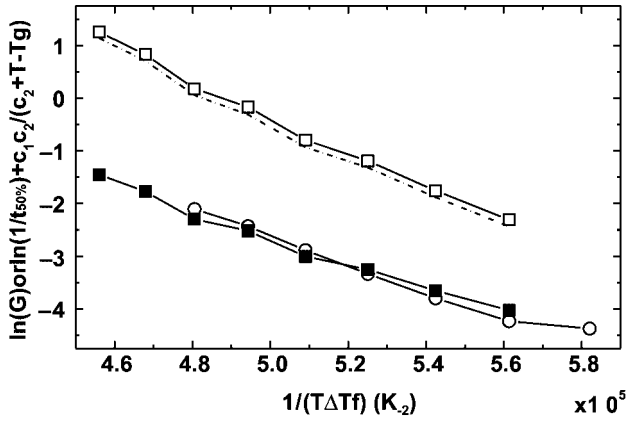

Figure 4. Representation of the $\ln(1/t_{50\%})$ in sec^{-1} (□), $\ln(G)$ in $\mathrm{mm\,sec}^{-1}$ (○) and the kinetic constant of Avrami's equation $\ln(k^{1/3})$ (- - -), with n equal to 3 vs. $1/T\Delta Tf$. The line with filled squares (■) is the shift of the experimental values of the $\ln(1/t_{50\%})$ subtracted by the number of nuclei per unit of volume at each crystallization temperature.

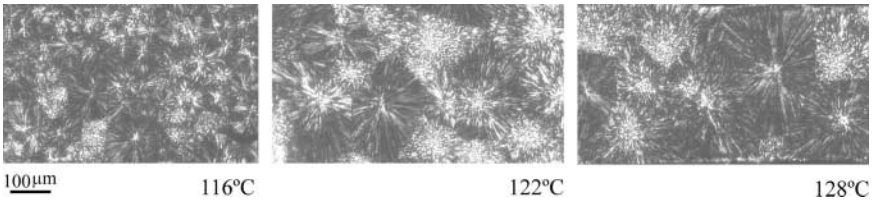

Figure 5. Spherulitic texture of sample's sections crystallized in the DSC at the indicated temperatures.

The numbers of nuclei at each crystallization temperature were evaluated according to Eq. (6), and the experimental data points of $\ln(1/t_{50\%})$ were corrected for the respective density of nuclei, yielding the line shown by black squares in Fig. 4. The absolute value of the slope of this new line is $2.431 \times 10^5\ K^2$, which is approximately the same as the slope of $\ln(G)$ vs. $(1/T\Delta Tf)$.

Several images of DSC crystallized sections, such as those shown in Fig. 5, were used to evaluate, by a direct counting, the number of spherulites and hence the number of nuclei. It may be observed that the boundary lines between spherulites is straight and that, in the field of view, their number decreases with increasing crystallization temperature. The density of nuclei as a function of the crystallization temperature is shown by the open circles in Fig. 6. The upper and lower dotted lines are the errors with which the measurements were performed. The solid line is the prediction of the average density of nuclei according to Eq. (6).

The nonisothermal crystallization data, shown in Fig. 7, were corrected for the calibration on cooling according to Eq. (10) (dotted line) and further corrected for the thermal resistance of the sample and the heat of crystallization released during

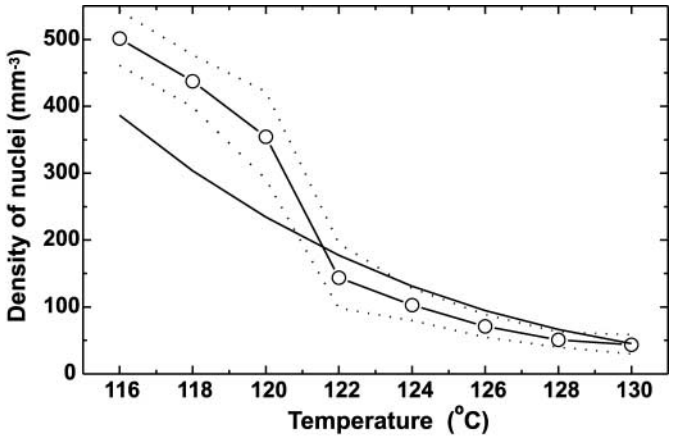

Figure 6. Experimental values of the density of nuclei plotted against the crystallization temperature (○). The top and bottom dotted lines are the errors with which the measurements were obtained. The solid line is the prediction of $\bar{N}_t$ according to Eq. (6).

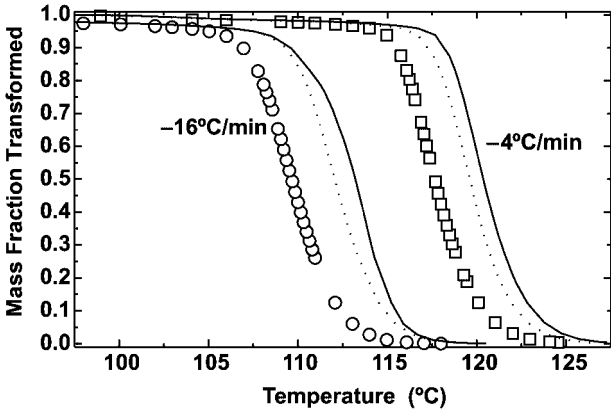

Figure 7. Nonisothermal crystallization of polypropylene at (○) −4°C/min and (□) −16°C/min. Dotted lines are the corrections for the calibration on cooling at the rates indicated. Solid lines are the corrections for the sample's thermal resistance and release of the heat of crystallization. The errors with which the calibration on cooling was performed at different rates are not shown in the figure: ±0.152°C for −4°C/min, ±0.626°C for −16°C/min, and ±1.6°C for −32°C/min.

solidification by Eq. (11) (solid line). The values of the parameters used in these corrections are those of Table 3. The slight bending in the experimental curves, resulting from the last temperature correction, and more evident for high cooling rates, is due to the release of the heat of crystallization.

From the corrected curves at several scanning rates, a temperature corresponding to half of the phase change was estimated. As may seen from Fig. 7, a significant amount of the phase change occurs in a temperature interval around $T_{50\%}$. An empirical relationship between $T_{50\%}$ and the cooling rate, established for the present situation, is

$$T_{50\%} = 105.669 + 13.751 \cdot \exp[-(\dot{T} - 4)/17.921] \tag{14}$$

The above relationship, together with the error bars resulting from the calibration on cooling, is shown in Fig. 8.

A microscopic analysis of the DSC sample sections, previously crystallized at specified cooling rates, allowed the experimental evaluation of the average density of

Table 3. Values of the parameters used by Eq. (11) for the evaluation of the average true sample temperature and $T_{50\%}$.

dT/dt (°C/min)	4	8	16	32
$\lvert\Delta H_c\rvert$ (J/g)	83.839	83.990	83.765	83.233
$T_{50\%}$ (°C)	119.6	116.3	112.96	108.49

R_s was 42.7°C/W, and the sample's thickness and diameter were 0.4 mm and 6.3 mm, respectively.

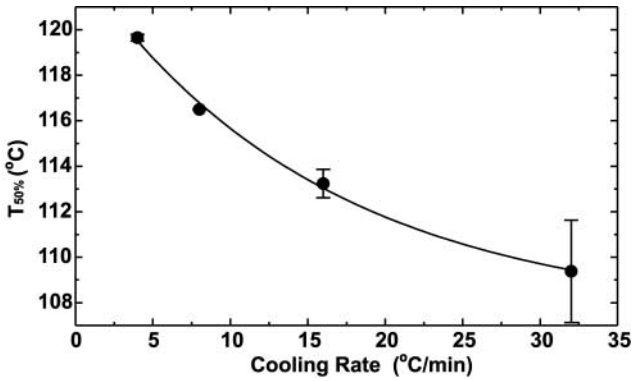

Figure 8. Variation of the temperature corresponding to 50% of the phase change against the cooling rate for nonisothermal experiments. Error bars are for the errors with which the calibration on cooling was performed and the solid line the fit to the experimental data according to Eq. (14).

nuclei (in a similar way to that used in Fig. 6). The results are shown by open squares in Fig. 9. For comparison, the experimental number of the average density of nuclei, obtained from isothermal experiments, is also shown (open circles on the right-hand side). The solid line is the predicted average density of nuclei from Eq. (6), with T equal to the isothermal crystallization temperature for isothermal scans and $T = T_{50\%}$ for the nonisothermal experiments. The error bars in this line are the effect of the error in the definition of $T_{50\%}$ (from the calibration on cooling) on the evaluation of the average density of nuclei.

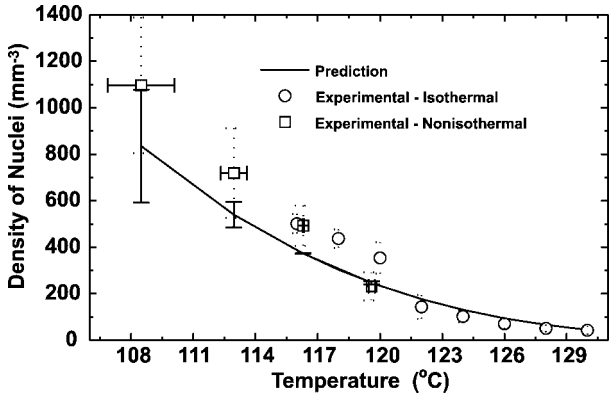

Figure 9. Experimental values of the density of nuclei plotted against the crystallization temperature measured for sample sections crystallized in the DSC at constant temperature (○) and for $T_{50\%}$, as measured from the curves of Fig. 7 after temperature corrections (□). The dashed horizontal error bar is for errors with which the calibration on cooling was performed (horizontal). The vertical errors bar (□) is for the errors in the counting of the number of nuclei. The solid line is the predicted value according to Eq. (6), and the solid error bars are the effect of the errors in the definition of $T_{50\%}$ over the prediction of the average density of nuclei.

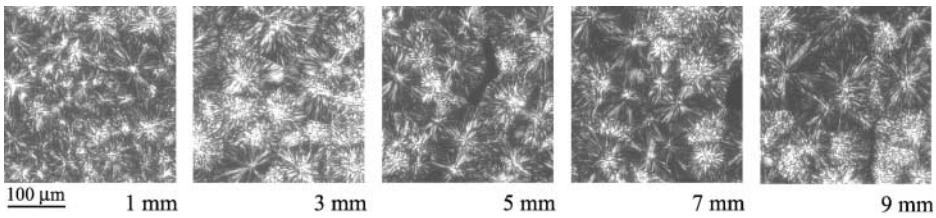

Figure 10. Spherulite texture of samples cut across the thickness of the polypropylene rotational molding.

The methodology used here for nonisothermal quiescent experiments was extended to the crystallization of polypropylene in rotational molding. From the data of Fig. 2, the cooling rates were evaluated, at different positions of the thermocouples across the thickness of the sample. They range from -4.7°C/min to -9.2°C/min at 9 mm and 3 mm from the mold surface, respectively. The value at 1 mm from the mold surface was obtained by extrapolation since, as shown in Fig. 2, the temperature profile at this position yielded a much lower cooling rate. This may have occurred due to thermocouple slippage during mold filling. Figure 10 shows cross-sections that were used for evaluating the nucleation density, and these were cut at the same positions where the thermocouples were located.

Inputting to Eq. (14), the values of the cooling rates at different positions through the thickness of the molding, the corresponding $T_{50\%}$ may be evaluated and, from this, the average density of nuclei may be determined by means of Eq. (6). Figure 11 shows the predicted and experimental values as a function of the cooling rate for the rotationally molded specimens. An alternative way to present this data is shown in Fig. 12, where the average spherulite diameter is plotted against the cooling rate. In this case, the predicted

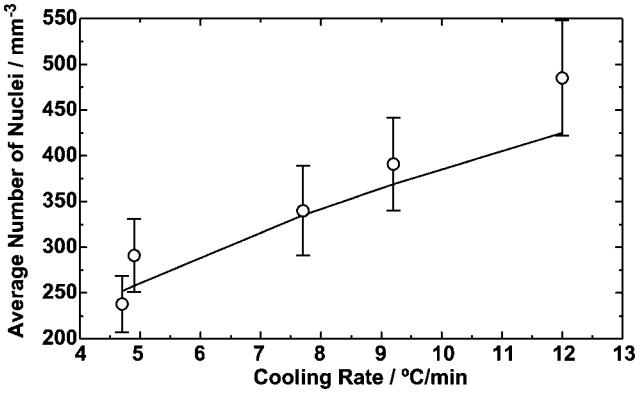

Figure 11. Average density of nuclei as measured from sample sections (○) and predicted from Eq. (6).

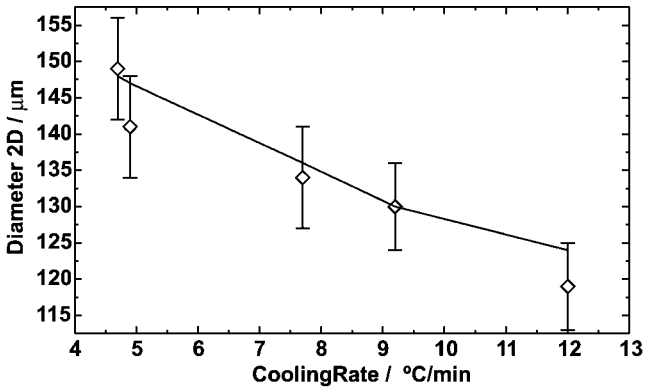

Figure 12. Measured average spherulite diameter (◇) and predicted value from the average density of nuclei of Fig. 11.

spherulite diameter is evaluated directly from the average density of the nuclei by assuming that they are spherical and occupy 100% of the volume.

DISCUSSION

The K_g^G value obtained from Fig. 4 ($2.689 \times 10^5\,K^2$) is comparable with the value obtained for regime III crystallization in isotactic polypropylene by Cheng and coworkers.[24] With Cheng's data, [$\sigma = 11.5\,erg/cm^2$, $\sigma_e = 52.3\,erg/cm^2$, $b_0 = 6.26\,Å$, $\Delta h_f = 8.3\,kJ/mol$, and $T_m^o = 176.75°C$ (measured for this material)], the value obtained for K_g^G is $2.634 \times 10^5\,K^2$. Furthermore, for isotactic polypropylene at temperatures below 137°C, the predominant regime is III,[25,26] which allows the prediction of the average density of the nuclei to be extended to lower temperatures ($\approx 108°C$ in this case), based on Eq. (6).

As stated previously, in the derivation and application of Eq. (6) for the prediction of the average density of nuclei, it was assumed that there is an instantaneous nucleation of spheres. Although this is a theoretical idealization, a nucleation activation process may be considered instantaneous when the rate of activation of nuclei is much larger than its growth rate. The experimental data obtained for this isotactic polypropylene suggest that this is a reasonable assumption. In particular, from the data of Fig. 3, an acceptable description of the isothermal crystallization at different temperatures was achieved with the Avrami exponent constant and equal to 3 for all crystallization temperatures. Also, images of molded cross-sections, such as those of Figs. 5 and 10, show straight boundary lines between neighbor spherulites. Finally, the ratio between $K_g^{1/t_{50\%}}/K_g^G$ is 1.253, compared with the theoretical value of 1.333. From all these results, one can conclude that the assumption of an instantaneous nucleation of spherical-shaped structures is acceptable for this material.

Deviation between the experimental value for the ratio $K_g^{1/t_{50\%}}/K_g^G$ and the expected one for an instantaneous nucleation of perfect spheres is probably due to the upper and lower columnar layers that always appear in specimens crystallized in the DSC. This may also be an

important source of error for the data shown in Figs. 6 and 9 at lower crystallization temperatures.

Additional factors, such as the co-monomer content and secondary crystallization, play a minor role in the definition of $t_{50\%}$ (or $T_{50\%}$). The first one is evaluated statistically during the isothermal crystallization, because $t_{50\%}$ is an average measure of the crystallization development. Secondary crystallization is disregarded due to its minor role in the formation of fully developed spherulites.

Concerning the results of the nonisothermal crystallization (Fig. 7), it is shown that the joint effects of the calibration on cooling, the thermal resistance of the sample, and the heat of crystallization released during solidification change the temperature scale, leading to a more realistic definition of the temperature corresponding to half of the phase change. This definition is important for an accurate evaluation of the average density of nuclei according to Eq. (6). After these corrections, the nonisothermal crystallization data may be modeled using Eq. (7) with data obtained from isothermal experiments.[17]

In previous work,[15] the errors involved in calibration on cooling were evaluated for several cooling rates, and it was assumed that the temperature corresponding to half of the phase change ($T_{50\%}$) is only affected by these errors, as shown in Fig. 8. Because of the difficulty in their evaluation, additional error sources, such as those related to the evaluation of the thermal resistance of the sample, were ignored at this stage.

Experimental values for the average density of the nuclei, found from nonisothermal experiments, follow those obtained from isothermal experiments (open squares and circles, respectively, in Fig. 9). The error bars with which the average density of nuclei is predicted from $T_{50\%}$ and Eq. (6), match those of the experimental average density of nuclei for these same experiments.

The prediction of the average density of nuclei for samples crystallized under real processing conditions, shown in Figs. 11 and 12, is in good agreement with the experimental value of the average density of nuclei and spherulite size. Another error source that may affect the predictions is the contraction during cooling, which for isotactic polypropylene is nearby 15%. Assuming that almost all the contraction occurs when the temperature reaches a value close to $T_{50\%}$ at the different sample layers, or thermocouple positions, the remaining errors in the evaluation of this temperature are those referred previously for nonisothermal DSC experiments. However, the extension of the method to samples crystallized at higher cooling rates may present some problems because of the difficulties in the evaluation of the errors for the calibration on cooling and the increase of the thermal lag between the top and bottom of the sample.

In practice, thermocouples would not be placed in the plastic to measure the temperature during the rotational molding cycle. The method used to control the process is to measure the temperature of the air inside the mold, which is related to the transformations that occur in the plastic during the cycle.[5] The cooling rate determined from this temperature measurement data, which is available in real time, is similar to the one experienced by the plastic at the inner surface of the part. It has been shown that very significant morphological changes occur at a small layer adjacent to this surface, depending on the processing conditions, and the nature of this layer has a major influence on the mechanical performance of the part under impact testing.[27] Thus, the prediction of the size of the spherulites at this layer is most important for predicting the mechanical properties of the molded part.

CONCLUSIONS

The procedure described here may be used to predict the average density of nuclei for polymers crystallizing under quiescent conditions in DSC equipment (either isothermal or nonisothermal). It may also be used under quiescent processing conditions, such as in rotational molding, if the cooling rate is known in different sections of the part being processed.

The basis of the methodology is a relationship between the spherulite growth rate data (obtained from optical microscopy) and half of the crystallization time (obtained from isothermal DSC experiments). The extension to nonisothermal crystallization requires evaluation of a temperature corresponding to half of the phase change, $T_{50\%}$, and its relationship with the cooling rate. The assumptions made are:

- constant crystallization regime in the temperature region where the experimental data are available and to the temperature region where they are being extrapolated to
- instantaneous nucleation
- the envelope of the solid structures have a spherical shape.

In the work carried out here, very good agreement was observed between the predicted data and measurements taken from rotationally molded polypropylene samples.

REFERENCES

1. Cottrell, A.H. *An Introduction to Metallurgy*, 2nd Ed.; Edward Arnold Ltd., London, UK. 1975.
2. Strudel, J.-L. In *Physical Metallurgy*, 3rd Ed.; Part II; Cahn, R.W., Haasen, P., Eds.; Elsevier Science Publishers BV: Amsterdam, 1983; Chap. 22.
3. Baltá Calleja, F.J. In *Structure Development During Polymer Processing*; Cunha, A.M., Fakirov, S., Eds.; Kluwer Academic Publishers, Serie E: Dordrecht, 2000; Vol. 370, 145.
4. Friedrich, K. Strength and fracture of crystalline isotactic polypropylene and the effect of molecular and morphological parameters. Prog. Colloid & Polym. Sci. **1978**, *66*, 299.
5. Crawford, R.J. *Rotational Molding of Plastics*; John Wiley & Sons Inc.: Chichester, 1996.
6. Cramez, M.C.; Oliveira, M.J.; Crawford, R.J. Effect of cooling rate and nucleating agents on the microstructure and properties of a rotational moulding grade of polypropylene. J. Mater. Sci. **2001**, *36*, 2151.
7. Martins, J.A.; Cruz Pinto, J.J.C. Evaluation of the instantaneous nucleation density in the isothermal crystallization of polymers. Polymer **2002**, *43*, 3999.
8. Cramez, M.C.; Martins, J.A.; Oliveira, M.J. Prediction of the average spherulite size in rotationally molded parts. EPS 2000 **2000**, *241*, 139.
9. Avrami, M.J. Granulation, phase change and microstructure. Kinetics of phase change III. J. Chem. Phys. **1941**, *9*, 177.

10. Evans, U.R. The laws of expanding circles and spheres in relation to the lateral growth of surface firms and the grain-size of metals. Trans. Faraday Soc. **1945**, *41*, 365.
11. Kolmogoroff, A.N. On the statistical theory of the crystallization in metals (in Russian). Izvest. Akad. Nauk. SSR., Ser. Math. **1937**, *1*, 335.
12. Hoffman, J.D.; Davis, G.T.; Lauritzen, J.I., Jr. In *Treatise on Solid State Chemistry*; Hannay, N.B., Ed.; Plenum Press: New York, 1976; Vol. 3, 497.
13. Kurz, W.; Fisher, D.J. *Fundamentals of Solidification*; Trans-Tech Publications, Switzerland, 1986.
14. Nakamura, K.; Watanabe, T.; Katayama, K.; Amano, T. Some aspects of non-isothermal crystallization of polymers. I. Relationship between crystallization temperature, crystallinity, and cooling conditions. J. Appl. Polym. Sci. **1972**, *16*, 1077.
15. Martins, J.A.; Cruz Pinto, J.J.C. The temperature calibration on cooling of differential scanning calorimeters. Thermochim. Acta **1999**, *332*, 179.
16. Crawford, R.J.; Nugent, P.; Xu, L. Computer prediction of the cycle times during rotational moulding of plastics. Adv. Polym. Tech. **1992**, *11*, 181.
17. Martins, J.A.; Cruz Pinto, J.J.C. The non-isothermal crystallization kinetics of polypropylene after DSC calibration on cooling. J. Macrom. Sci.–Physics **2000**, *35*, 711.
18. Martins, J.A.; Cruz Pinto, J.J.C. *True Sample Temperature in Isothermal Scans*, Thermodynamics, O7; 12th ICTAC: Copenhagen, 2000; 172.
19. Van de Weygaert, R. Fragmenting the universe. III. The construction and statistics of 3-D Voronoi tessellations. Astron. Astrophys. **1994**, *283*, 361.
20. Eder, G.; Janeschitz-Kriegl, H. In *Materials Science and Technology*; Meijer, H.E.H., Ed.; Verlag Chemie: Weinheim, 1994; Vol. 18; Chap. 4.
21. Guo, X.; Isayev, A.I.; Demiray, M. Crystallinity and microstructure in injection mouldings of isotactic polypropylenes. Part II. Simulation and experiment. Polym. Eng. Sci. **1999**, *39*, 2132.
22. Eder, G.; Janeschitz-Kriegl, H.; Liedauer, S. Crystallization processes in quiescent and moving polymer melts under heat transfer conditions. Prog. Polym. Sci. **1990**, *15*, 629.
23. Crawford, R.J.; Nugent, P. New process control system for rotational moulding. Plast. Rubb. Comp. Proc. Appl. **1992**, *17*, 23.
24. Cheng, S.Z.D.; Janimak, J.J.; Zhang, A. Regime transitions in fractions of isotactic polypropylene. Macromolecules **1990**, *23*, 298.
25. Galeski, A. In *Polypropylene: Structure, Blends and Composites*; Karger-Koscis, J., Ed.; Chapman & Hall: Cambridge, England, 1995; Chap. 4.
26. Monasse, B.; Haudin, J.M. Growth transition and morphology change in polypropylene. Colloid & Polymer Sci. **1985**, *263*, 822.
27. Oliveira, M.J.; Cramez, M.C.; Crawford, R.J. Structure–properties relationship in rotationally moulded polyethylene. J. Mater. Sci. **1996**, *31*, 2227.

Received August 13, 2001
Revised May 20, 2002
Accepted May 27, 2002